THE JOURNAL OF PHYSICAL CHEMISTRY B
A JOURNAL OF THE AMERICAN CHEMICAL SOCIETY

pubs.acs.org/JPCB

Article

Correlated Fluctuations of Structural Indicators Close to the Liquid–Liquid Transition in Supercooled Water

Published as part of The Journal of Physical Chemistry virtual special issue "Pablo G. Debenedetti Festschrift".

Riccardo Foffi and Francesco Sciortino*

Cite This: https://doi.org/10.1021/acs.jpcb.2c07169

Read Online

ACCESS | Metrics & More | Article Recommendations | Supporting Information

ABSTRACT: Multiple numerical studies have unambiguously shown the existence of a liquid–liquid critical point in supercooled states for different numerical models of water, and various structural indicators have been put forward to describe the transformation associated with this phase transition. Here we analyze numerical simulations of near-critical supercooled water to compare the behavior of several of such indicators with critical density fluctuations. We show that close to the critical point most indicators are strongly correlated to density, and some of them even display identical distributions of fluctuations. These indicators probe the exact same free energy landscape, therefore providing a thermodynamic description of critical supercooled water which is identical to that provided by the density order parameter. This implies that close to the critical point, there is a tight coupling between many, only apparently distinct, structural degrees of freedom.

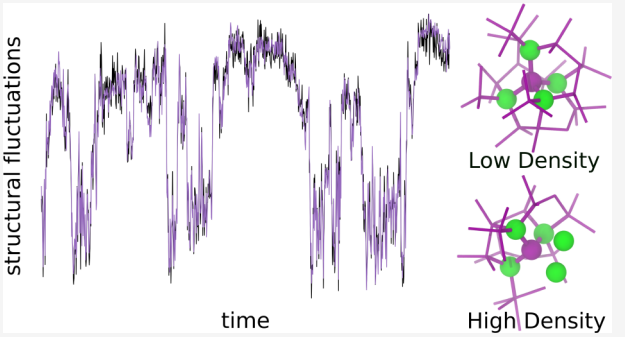

INTRODUCTION

Water has an intriguing thermodynamic behavior, which originates from its ability to alter its local structure in response to changes in pressure and temperature. The tetrahedral geometries characteristic of crystalline ice persist, locally, also in the liquid state, but depending on the external conditions, the hydrogen bond (HB) network of water can undergo drastic rearrangements, leading to significant distortions in the local environment.[1,2] The thermodynamic anomalies of liquid water are therefore a direct result of the peculiar properties of the HB network, where local rearrangements are accompanied by an anticorrelation between local density and local energy, in stark contrast to the behavior of normal liquids.[3]

One of the most striking consequences is polyamorphism, the existence of multiple distinct amorphous phases for a single-component substance.[4,5] In particular, two of these, the low-density amorphous (LDA) and high-density amorphous (HDA) phases, appear to be separated by a first-order transition.[6−8] On the basis of numerical simulations, Poole et al.[9] advanced the suggestive hypothesis that the LDA-HDA first-order transition could be the kinetically arrested manifestation of a liquid–liquid transition (LLT), occurring at deeply supercooled conditions and involving two distinct, metastable liquid states, a low- and a high-density liquid (LDL and HDL). This LLT line would terminate at a liquid–liquid critical point (LLCP). Despite many controversies,[10,11] cutting-edge experimental efforts are now entering in the no-mans land,[12−16] providing increasingly stronger hints at the possibility that the LLT actually exists in real water.[14] In many numerical models of water, however, a LLT has been predicted to exist,[9,17−21] including models based on neural network potentials[22] and models including quantum nuclear effects.[23] In other models, the existence of a liquid–liquid critical point has been rigorously proven.[24−30] In silico, a liquid–liquid critical point has also been clearly identified in colloidal models mimicking, at the nano- and micron-scale, the tetrahedral binding of water.[31−34]

Insight into the properties of water can be gained through the use of two-state models,[35−41] where (with some variations and subtleties) water is seen as a binary mixture of two competing and continuously interconverting local structures. There is, in particular, a tradition of classifying the molecular components of the liquid in terms of "structural indicators", quantities that assign a scalar value to each molecule on the basis of local structural (or energetic) properties,[36,42−49] allowing a distinction between structures that appear more LDL-like or HDL-like. More recently, further structural insight is also being provided by explicitly analyzing the topological

Received: October 12, 2022
Revised: December 1, 2022

properties of the HB network[50−52] and other graph-theoretical approaches.[53] A few studies tried to perform a comparison of certain aspects of structural indicators,[54,55] but unfortunately not in the critical region of supercooled water.

One of the most prominent signatures of proximity to a critical point is the onset of critical density fluctuations, whose distribution is tightly related to the free energy landscape of the system.[56] Performing numerical simulations of water close to the LLCP, these fluctuations can be probed, highlighting continuous crossovers between the two liquid states.[29] It is interesting, in these conditions, to assess what other physical properties of the system are affected by the critical phenomenon, and to what extent these structural indicators are correlated to the density.

In this work we analyze tenths-of-μs-long molecular dynamics trajectories to explore how the presence of critical density fluctuations in supercooled water correlates to the behavior of structural indicators. We find that most commonly used structural indicators display a near-perfect correlation with the density, implying the existence of a tight coupling between the structural properties to which they are sensitive. Moreover, we find that some of the indicators show identical distributions of fluctuations close to the LLCP, leading to equivalent descriptions of the free energy landscape: density or any single one of these indicators are sufficient to completely (and identically) describe the thermodynamics of the LLT. Away from the LLCP, as the standard component of the free energy overcomes the critical one, the coupling between the different structural indicators is weakened and a one-to-one relationship to the density cannot be established anymore for most of them.

METHODS

Molecular dynamics simulations of TIP4P/Ice water[57] were performed in the NPT ensemble using GROMACS 5.1.4[58] in single precision. Integration of the equations of motion was performed with a leapfrog integrator with time step 2 fs, temperature coupling was controlled by a Nosé−Hoover thermostat[59] with characteristic time 8 ps, and pressure coupling was controlled by an isotropic Parrinello−Rahman barostat[60] with characteristic time 18 ps. Molecular constraints were implemented by a sixth-order LINCS algorithm.[61] A cutoff distance 0.9 nm was selected for van der Waals forces and electrostatic interactions were evaluated with a fourth-order particle-mesh Ewald method,[62] with a real-space cutoff of 0.9 nm. The main analysis was performed in the inherent structures[63] (unless specified otherwise), obtained by minimization of the potential energy via the steepest descent algorithm (STEEP) in GROMACS, in double precision, with a force tolerance of 1 J mol^{-1} nm^{-1} and a maximum step size of 5×10^{-4} nm. Some of the analyses were also based on real dynamics trajectories.

70 μs long simulations at 188 K, 1675 bar, close to the critical point of TIP4P/Ice (estimated at 188.6 K and 1725 bar[29]), probing the critical density fluctuations, were performed with a small system of 300 molecules, sampling configurations at intervals of 40 ns. Other simulations, used to explore the behavior of structural indicators along isobars, were performed with 1000 molecules. In this case, the simulated time was longer than 40 μs at the lowest temperatures and configurations were sampled at intervals of 80 ns.

The presence of a H-bond between two water molecules was assessed following the definition by Luzar and Chandler;[64] this information is needed to evaluate some of the structural indicators. According to this definition, two H_2O molecules are H-bonded if their O···O distance is less than 3.5 Å and their $\hat{HOO}$ angle (the minimal angle between the intramolecular OH bond and the intermolecular O···O line) is less than 30°. It was shown in refs 51 and 52 that this geometric definition is highly accurate over a wide range of conditions in supercooled TIP4P/Ice water (including conditions investigated herein), especially if performed on the inherent structures, in which thermal fluctuations have been removed.

STRUCTURAL INDICATORS

A structural indicator $\mathcal{I}$ assigns a scalar value to each molecule depending on its local environment, a value that can be interpreted as the "level of order" associated with the local structure, where the loose definition of order indicates, in analogy with the ice structure, the propensity to form open, tetrahedrally coordinated, local structures. These open tetrahedral local arrangements are favored at low temperature and low densities, and hence, in broad terms, density is negatively correlated with local order. Some of the indicators are positively correlated with order (i.e., they assign high values to highly ordered configurations); others have a negative correlation. For convenience, in the following analysis we will deliberately multiply all studied indicators by a factor $\epsilon_{\mathcal{I}} = \pm 1$ so that after the multiplication all of them are positively correlated with order: low values of $\epsilon_{\mathcal{I}}\mathcal{I}$ represent disordered structures (more HDL-like), and high values of $\epsilon_{\mathcal{I}}\mathcal{I}$ indicate ordered structures (LDL-like).

In this article we compare density and a comprehensive set of structural indicators, listed below.

- q_4[44] is a measure of angular ordering, representing the level of tetrahedrality of the local structure around a selected molecule in terms of the angular arrangement of its four closest neighbors.
- d_5[36] is the (oxygen−oxygen) distance of a molecule from its fifth-nearest neighbor; it has been suggested that d_5 generally overestimates the level of order in the local structures.[39]
- LSI (Local Structure Index)[45] is a radial measure of the variance of intermolecular distances between successive neighbors.
- ζ[46] is the first parameter to explicitly account for H-bonding; it measures the distance between the nearest non-H-bonded and farthest H-bonded molecule, providing a measure of shell interpenetration. A particularly convenient property of ζ is the possibility to represent its distribution as the superposition of two Gaussian curves.
- V_4[48] is the only energy-based descriptor in the set: for each molecule, all its pairwise interaction energies are evaluated and ranked based on their strength; V_4 is the energy associated with the fourth-strongest interaction. V_4 is expected to correspond to the typical linear HB energy in a local tetrahedral configuration, becoming weaker (less negative) when structural distortions are introduced. It correlates positively with density.
- NTC (Node Total Communicability)[53] is a recently introduced graph-theoretical metric of the cumulative connectivity of each water molecule, highlighting the contribution of intermediate/long-range effects; it was found to be particularly sensitive to variations in high-density structures. High values of NTC represent high

https://doi.org/10.1021/acs.jpcb.2c07169
J. Phys. Chem. B XXXX, XXX, XXX−XXX

connectivity and higher values of density. It must be noted that links in the network are defined on the basis of a simple geometric oxygen−oxygen distance criterion, so the resulting connectivity pattern does not coincide with the HB network.

- Another recent topological indicator is the centerline helicity $\mathcal{H}_c$, a measure of the "degree of entangledness" in the HB network based on the identification of knots and ring structures.[34]
- Finally, we also present data based on a novel indicator, Ψ, introduced here for the first time. Recent studies[51,52] have shown that molecules at chemical distance $D = 4$ (i.e., pairs of molecules separated by 4 links along the HB network) are characterized by typical distances that are very different between the LDL and HDL phases. In the LDL phase, these molecules are typically at large distances $r \approx 6$ Å. In the HDL, instead, there is a significant probability of detecting these chemically distant pairs of molecules at close distances in real space, constituting interstitial pairs ($r \approx 3.5$ Å). The value of Ψ of a molecule m is defined as the minimal real-space distance between molecules at chemical distance $D = 4$ from m. Further details on the definition of Ψ are reported in the Supporting Information, and a simple Julia script for the evaluation of Ψ has been made available via GitHub.[65]

All these indicators quantify local properties of single molecules, associating a value $\mathcal{I}^{(m)}$ to each molecule m. To associate a value to each configuration we can evaluate a system-level (or global) indicator by averaging over all molecules (N) in the sample: $\mathcal{I} = \sum_{m=1}^{N} \mathcal{I}^{(m)}/N$. The time sequence $\mathcal{I}(t)$ of each global indicator, a measure of the time evolution of the average structural properties, can be correlated to density and to any other distinct structural indicator.

RESULTS AND DISCUSSION

Figure 1A displays critical density fluctuations over a time scale of several μs observed in a constant-pressure molecular dynamics simulation of TIP4P/Ice water at $T = 188$ K, $P = 1675$ bar, a state point close to the model's critical point (188.6 K and 1725 bar).[29] In this condition, the density oscillates between values typical of the low- and the high-density liquid. Also the time evolution of structural indicators is characterized by wide fluctuations around two distinct average values, with frequent flips between the two, as shown in Figure 1B,C for $+\zeta$ and $+\Psi$, revealing that these indicators can detect the critical fluctuations; the same is true for all the other indicators considered here.

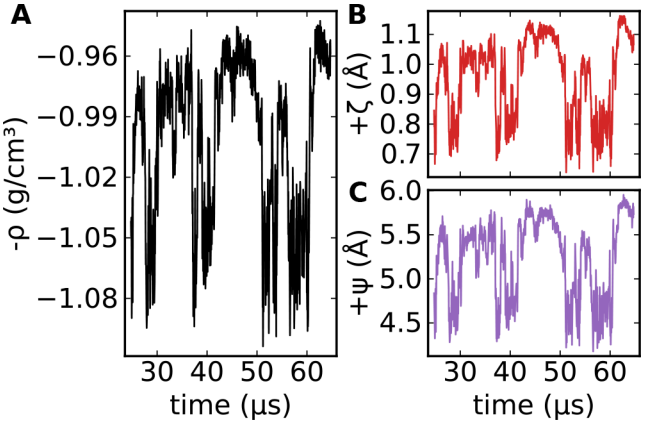

Figure 1. Time dependence of the (negative of the) density (A) and system-averaged structural indicators (B,C) from a constant-pressure simulation of TIP4P/Ice simulations at $T = 188$ K, $P = 1675$ bar (a state point close to the liquid−liquid critical point), and $N = 300$ molecules. The figure shows wide fluctuations between two distinct average values over μs time scales.

To quantify the ability of the investigated structural indicators to identify critical fluctuations (as detected by the oscillation in the system density) we define the fluctuation of a global indicator $\mathcal{I}$ as

$$\delta\mathcal{I} = \frac{\mathcal{I} - \langle\mathcal{I}\rangle}{\sqrt{\langle(\mathcal{I} - \langle\mathcal{I}\rangle)^2\rangle}} \tag{1}$$

where $\langle\cdot\rangle$ denotes a time average. The resulting quantities $\delta\mathcal{I}$ are dimensionless, all with zero mean and unit variance, allowing a direct comparison between the behavior of distinct structural indicators and density fluctuations. Figure 2 shows the time dependence of $\delta\mathcal{I}$ for all investigated indicators, each of them superimposed with the density fluctuations ($-\delta\rho$). In proximity of the LLCP, all the structural indicators we considered show a near-perfect correlation with the critical density fluctuations and between themselves.

The correlation between any two quantities $\mathcal{I}_i$ and $\mathcal{I}_j$ is quantified by the Pearson correlation coefficient

$$r(\mathcal{I}_i, \mathcal{I}_j) = \langle\delta\mathcal{I}_i\delta\mathcal{I}_j\rangle \tag{2}$$

where $\langle\cdot\rangle$ is a time average. The resulting correlation coefficients (between density and structural indicators and between pairs of structural indicators) are reported in Figure 3. All quantities are highly correlated with density ($r > 90\%$), with d_5, ζ, Ψ, and LSI above 98%. The indicators that less correlate with density (but still >90%) are V_4 and NTC, which also show slightly weaker correlations with the other indicators. This is not really surprising given that they are not explicit descriptors of local structure but rather of energy and "connectivity". Still, the extremely high values of the correlation coefficients tell us that all these distinct structural properties are strongly coupled: any variation in system density is accompanied by a perfectly concerted response of only apparently distinct structural features. We note in particular that d_5, LSI, and ζ are intercorrelated at $r \geq 99.8\%$.

Figure 4A shows the distribution of fluctuations displayed by all investigated global structural indicators. Most of them almost exactly match the distribution of density fluctuations. The exceptions are NTC and V_4, which are sampled from different distributions (as verified by a Kolmogorov−Smirnov test[67] at 95% confidence, with $p = 0.048$ for V_4 and $p < 10^{-9}$ for NTC). Since the (logarithm of the) probability distribution in any observable is related to the system free energy, expressed as a function of the same observable, then Figure 4A confirms that all the analyzed indicators, except NTC and V_4, represent essentially the same free energy profile. In other words, they provide—close to the LLCP—the exact same thermodynamic description of the system as the density. All the structural changes that are picked by the different structural indicators are so strongly coupled among themselves (and with density) that, thermodynamically speaking, each of them could be equally well selected as order parameter for the LL transition. At the same time, these results suggest that, close to

https://doi.org/10.1021/acs.jpcb.2c07169
J. Phys. Chem. B XXXX, XXX, XXX−XXX

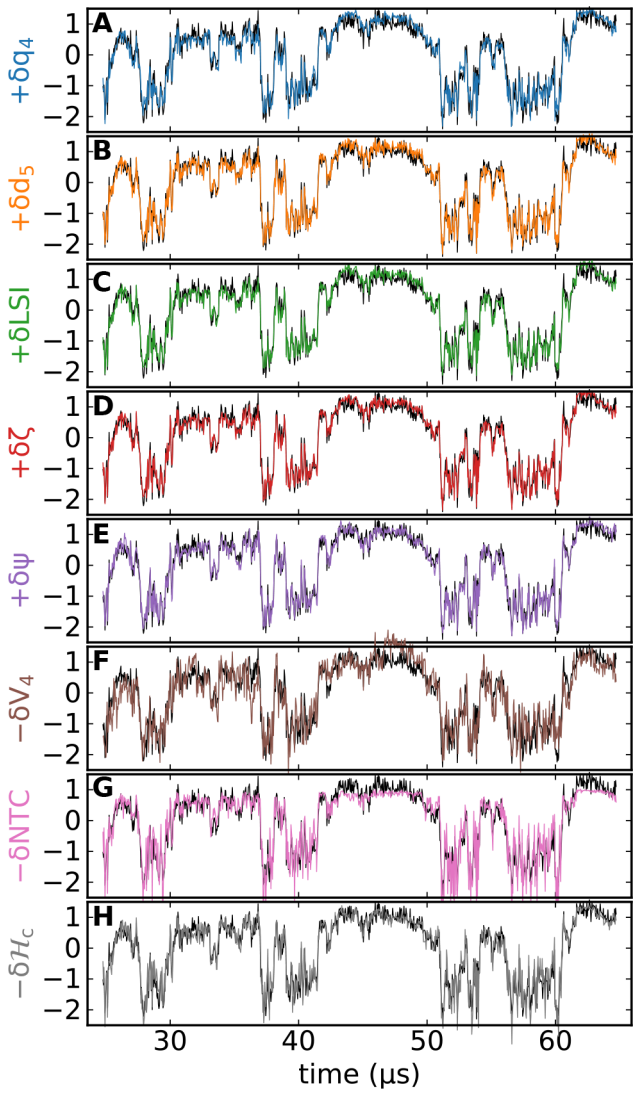

Figure 2. Critical density fluctuations ($-\delta\rho$, black) compared to fluctuations of the structural indicators (color-coded): all indicators correlate strongly with density fluctuations in proximity of the critical point in TIP4P/Ice. Data from TIP4P/Ice simulations at T = 188 K, P = 1675 bar, and N = 300 molecules.

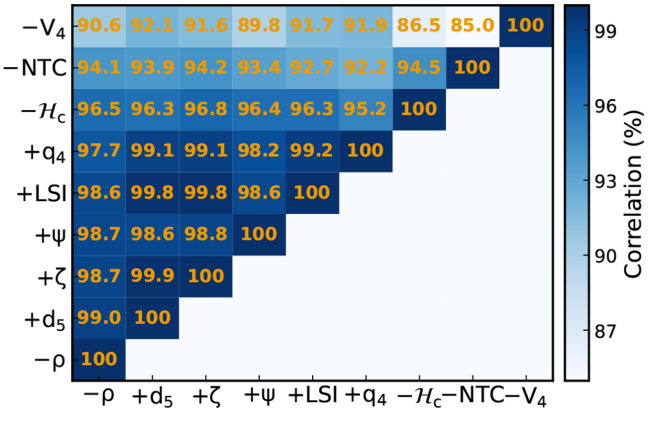

Figure 3. Pearson correlation coefficients between density and structural indicators and between pairs of structural indicators. Indicators are sorted, left to right and bottom to top, by their correlation with density. Data from TIP4P/Ice simulations at T = 188 K, P = 1675 bar, and N = 300 molecules.

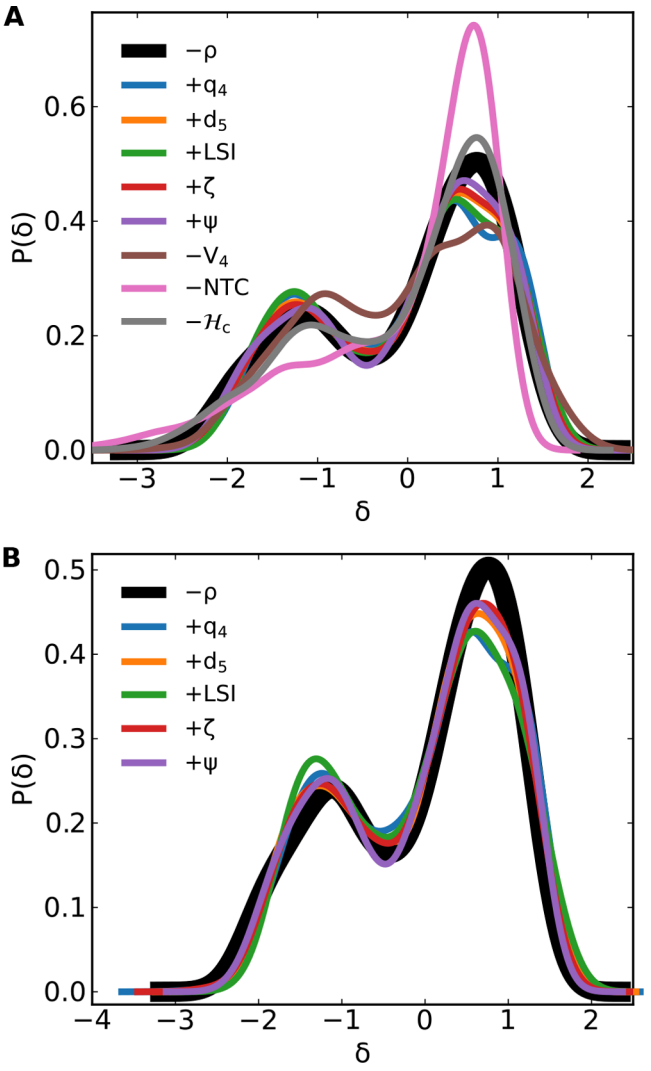

Figure 4. Distribution of density (black, thick) and system-level structural fluctuations (eq 1, color-coded) close to the critical point in TIP4P/Ice water, T = 188 K, P = 1675 bar, N = 300. Curves obtained from kernel density estimations[66] from data calculated in the inherent structure configurations (A) and in the real dynamics (B, only for some of the indicators). All the quantities that showed global bimodal distributions in the inherent structures (Figure 4) retain the bimodality also in the real dynamics. Except for NTC and V_4, all quantities are described by the same distribution.

the LLCP, structural indicators do not provide additional information as compared to density.

We also verified that the same conclusions can be reached by performing the analysis in the real dynamics, instead of the inherent structures. Indeed, the global indicators which displayed a bimodal distribution of fluctuations in the inherent structures also retain this bimodality in the real dynamics (Figure 4B). This is consistent with the fact that the process of energy minimization only removes thermal noise from the system, without affecting the underlying free energy profile.

We highlight that a large correlation coefficient does not per-se imply that the distributions of the fluctuations are identical. Consider the case of NTC. Figure 2G shows that while the density jumps from LDL to HDL are rather well followed by δNTC, the amplitude of the fluctuations inside the LDL and the HDL basins are not properly reproduced. In the LDL basin (high δ) the fluctuations are less intense, resulting in a higher

https://doi.org/10.1021/acs.jpcb.2c07169
J. Phys. Chem. B XXXX, XXX, XXX−XXX

peak in the distribution, while in the HDL fluctuations inside the basin are amplified compared to those of ρ, resulting in large fluctuations that are too spread-out to produce a peak (i.e., same-density configurations can result in different NTC values, implying a sensitivity to some property which is distinct from ρ). In summary, q_4, d_5, LSI, ζ, Ψ, and $\mathcal{H}_c$ not only provide an accurate estimate of the flipping between LDL and HDL configurations but also properly model the fluctuations inside each of these two basins.

We have observed that system-averaged indicators $\mathcal{I}$ can detect the transition and some of them even reproduce the correct free energy profile; it is now interesting to investigate whether the transition can also be detected by the molecular-level indicators, $\mathcal{I}^{(m)}$. For each molecule m we evaluate its fluctuation (dimensionless, with zero mean and unit variance) as

$$\delta_m \mathcal{I}(t) = \frac{\mathcal{I}^{(m)}(t) - \overline{\mathcal{I}}}{\sqrt{\langle (\mathcal{I}^{(m)}(t) - \overline{\mathcal{I}})^2 \rangle_{m,t}}} \tag{3}$$

where $\overline{\mathcal{I}} = \langle \mathcal{I}^{(m)}(t) \rangle_{m,t}$ and $\langle \cdot \rangle_{m,t}$ is an average over all molecules m in the system and all times t. The values of $\delta_m \mathcal{I}(t)$ for each molecule m at each time t are then pooled together to obtain the distribution of molecular-level structural fluctuations, shown in Figure 5 for the four indicators d_5, LSI, ζ, and

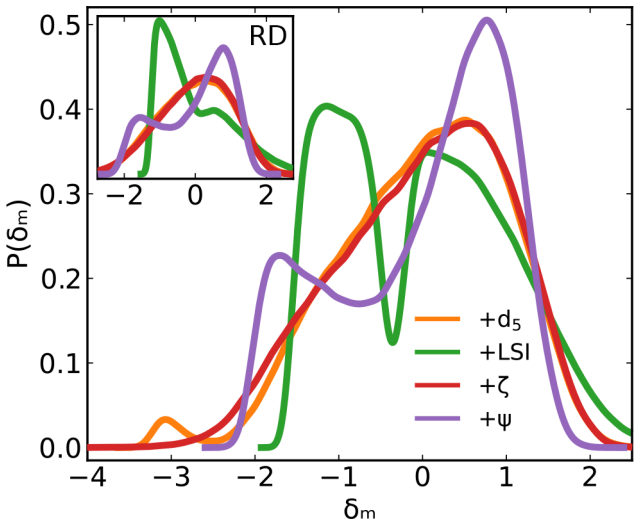

Figure 5. Zero-average and unit variance distribution of structural indicators evaluated at the molecular level (δ_m, eq 3) in the inherent structure configurations. Inset: same distributions evaluated from configurations in the real dynamics. Only LSI and Ψ show molecular-level bimodality, and only Ψ retains this bimodality also in the real dynamics. Data from TIP4P/Ice simulations at T = 188 K, P = 1675 bar, and N = 300 molecules.

Ψ. Despite the proximity of the critical point and the sampling of both LDL and HDL configurations, here ζ and d_5 display (almost identical!) broad unimodal distributions. LSI and Ψ show, instead, clear bimodality, indicating the apparent ability of these two indicators to discriminate quite efficiently the two different local environments. The result for LSI is consistent with previous observations.[68−70] Interestingly, Ψ (and only Ψ) retains its distinct bimodal character even when configurations from the real dynamics (as opposed to the inherent structures) are used to evaluate δ_m (Figure 5 inset). In the real dynamics, LSI still shows two peaks but they are not as well-separated as in the inherent structures, a known result that called attention to the possibility that energy minimization could lead to improper characterization of local structures.[47] The fact that the indicator Ψ, which includes information from four successive HBs (which can span distances from 3 up to 7 Å), retains its bimodality also in the real dynamics, suggests instead that thermal-noise-resilient indicators require the selection of structural properties that sample an extended local region, and that energy minimization is not fundamentally affecting the structure of the liquid.

In studying the LSI distribution we found that its shape (especially at molecular level) is strongly dependent on the choice of the threshold distance, which is used in its definition (as already partially observed by Accordino et al.[71]). The bimodality of the global indicator in the inherent structures is preserved for several threshold distance values, but the area under each peak (and hence the fraction of molecules in low- and high-density local configuration) is strongly threshold-dependent. The extreme sensitivity to this threshold at the single-molecule level calls for additional care when using LSI to perform local structural analysis (see further discussion in the Supporting Information, Figure S1).

Molecular level correlations between different pairs of indicators can be analyzed by means of their joint probability distributions (Figure 6); a one-to-one correspondence between two indicators would be represented by a clean monotonic relationship. This is the case for ζ and d_5 (Figure 6A) displaying an almost perfect linear correlation, apart from the very few points with $d_5 \lesssim 3$ Å, signaling the presence of a few molecules with five HBs in LDL-like environments. A strong correlation is also observed between ζ and LSI (Figure 6B) and between LSI and d_5 (Figure 6C) (with the same caveat for the $d_5 \lesssim 3$ Å molecules). The sharp discontinuity in Figure 6C around $d_5 \approx 3.7$ Å is, again, an artifact from the threshold used in the evaluation of LSI (which is exactly 3.7 Å in the canonical definition); this effect is discussed in the Supporting Information, where we also show that the location of this discontinuity always corresponds to the threshold in the LSI definition (Figure S2).

Looking at Ψ vs ζ (Figure 6D) we discover, instead, two clearly different basins, one 0.5 Å $\lesssim \zeta \lesssim$ 1 Å and $\Psi \lesssim$ 4 Å, and one for $\zeta \gtrsim 1$ and $\Psi \gtrsim 5$ Å; the existence of two distinct basins suggests that these two indicators are not tightly correlated at the molecular level. The bimodality of Ψ highlights the underlying bimodal structure of ζ, which is "masked" by the distance between the two basins being small with the respect to their width.

To provide evidence that the two basins in Figure 6D are indeed associated with the LDL and HDL configuration, we show in Figure 7 the corresponding quantities evaluated in both LDL and HDL close to coexistence at P = 1800 bar and T = 188 K (in a system with 1000 molecules). In this case, critical fluctuations are missing and each trajectory samples only one of the two basins. As expected, the LDL liquid has a strong peak at $\Psi \approx 6$ Å at $\zeta \gtrsim 1$ Å, while the HDL liquid has a strong peak at the interstitial distance $\Psi \approx 3.5$ Å and $\zeta \approx 0.5$ Å.

Finally we explore if the observed correlations close to the critical point survive also far from it, when the noncritical part of the free-energy plays a dominant role. Figure 8A shows the density−temperature relationship for four different isobars. At ambient pressure density decreases on cooling, and at 2500 bar density slightly increases on cooling. Figure 8B shows instead

https://doi.org/10.1021/acs.jpcb.2c07169
J. Phys. Chem. B XXXX, XXX, XXX−XXX

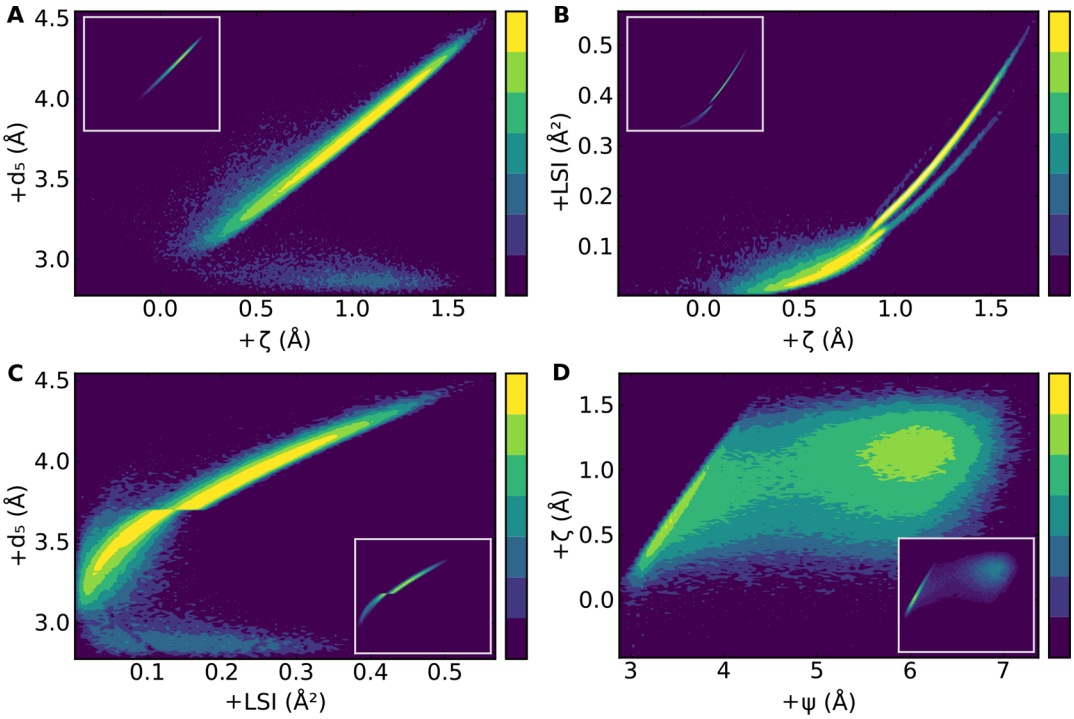

Figure 6. Joint probability distributions for selected pairs of structural indicators in TIP4P/Ice close to the critical point. For each molecule, d_S, LSI, and ζ are in a nearly perfect one-to-one relationship to each other (A–C); other indicator pairs, like ψ–ζ (D) do not have this property. Distributions are obtained by collecting together the indicator values for each molecule in the system at each time step. Main panels show the distribution in logarithmic scale to accentuate features, with each color level corresponding to an order of magnitude increase in relative frequency. Insets show the same distributions in linear scale. Data are from TIP4P/Ice simulations at T = 188 K, P = 1675 bar, and N = 300 molecules.

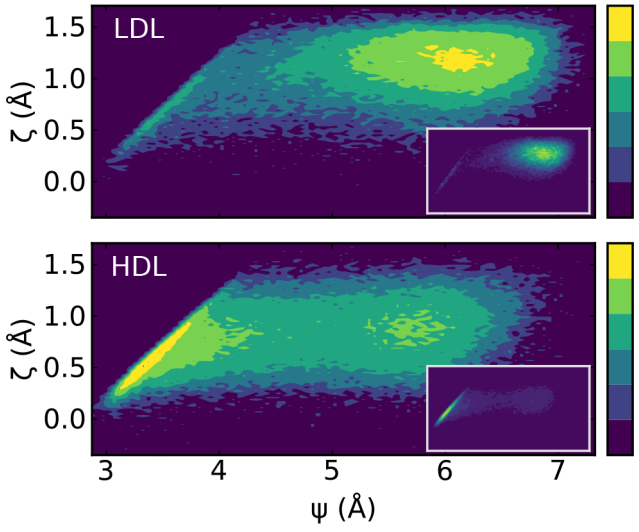

Figure 7. Correlation map between ζ and ψ in LDL and HDL close to coexistence: logarithmic colormap in main panel with each level corresponding to an order of magnitude increase in relative frequency, linear colormap in inset. Data are from TIP4P/Ice simulations at T = 188 K, P = 1800 bar, and N = 1000 molecules (from ref 52). Due to the proximity to coexistence, the simulation started in the low-density (high-density) liquid phase never crosses to the high (low) phase during the numerical study.

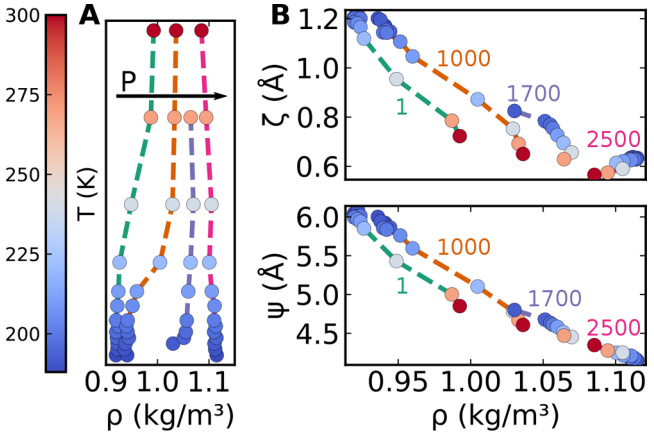

Figure 8. Structural indicators away from the LLCP are not in a one-to-one relationship with density. (A) Four isobars (1, 1000, 1700, and 2500 bar from left to right) in the T–ρ phase diagram. (B) Evolution of structural indicators ζ and ψ as a function of density along the four isobars shows a residual dependency, unique for each indicator, on temperature and pressure. In all panels isobars follow the same color-coding and marker colors represent temperature according to the colorbar on the left.

the density dependence of the time-averaged value of global indicators $\mathcal{I}$ (selecting ζ and Ψ as examples) as a function of the average density. If a state-point-independent correlation existed, all points would lie on the same curve. The observation of different functional forms suggests that away from the LLCP, the identity between global structural indicators ($\mathcal{I}$) and density (and between different structural indicators) is lost; along the different isobars, there is not a one-to-one correspondence between ρ and the indicators. The ζ–ρ relationship has significant nonlinearities. In particular, along the 2500 bar isobar, the dependency of ζ on ρ is inverted: at that pressure, ρ is slightly decreasing with increasing T; ζ, which at lower pressures is negatively correlated to ρ, becomes

https://doi.org/10.1021/acs.jpcb.2c07169
J. Phys. Chem. B XXXX, XXX, XXX–XXX

now positively correlated to it, showing itself a slight decrease (and hence a decrease in order). Interestingly, we note that the relation $\Psi-\rho$ is instead much more linear and does not show the same inversion observed in $\zeta-\rho$: even at high P, Ψ is always negatively correlated to ρ, suggesting that the correlation between Ψ and ρ holds in a large phase-space region.

CONCLUSIONS

In thermodynamics and classical theories of liquid state, the relevant order parameter to describe the gas−liquid transition in single-component fluids is density (ρ).[72] The LLT belongs, like the gas−liquid transition, to the universality class of the 3D Ising model,[73] so it must be described by a scalar order parameter. Recent numerical results[24,29,30] provide support to the hypothesis that even in the liquid−liquid transition, density (augmented by an energy correction, the so-called field mixing effect[74]) plays the same role as magnetization in the Ising model. As a caveat, we must note that it is possible to design a model where phases with the same density but different fractions of local motifs coexist; in these ad hoc cases ρ cannot be used as an order parameter for the liquid−liquid transition.[41]

There have been, however, also proposals for a two-order-parameter theory of water,[75−77] expressing the liquid free energy in terms of ρ and of an additional scalar nonconserved parameter, a structural indicator. It has been also argued that the density is the order parameter relevant for the gas−liquid transition, whereas a structural order parameter is relevant for the liquid−liquid transition.[77] In this view, the difference in density between HDL and LDL is a consequence of the intrinsic density difference of the two local structures.[77]

Here, analyzing molecular dynamics simulations of the TIP4P/Ice water model close to its liquid−liquid critical point, we compared critical density fluctuations to the structural fluctuations as described by different structural indicators (q_4, d_5, LSI, ζ, V_4, NTC, and a newly defined Ψ). Our analysis shows that all these indicators are capable of detecting, with high accuracy, transitions between the two liquid states, showing a near-perfect correlation to density and also to other indicators (Figures 2 and 3). Furthermore, we observed that most of them display the same distribution of fluctuations as the density, implying that they probe the same free energy landscape (Figure 4). Therefore, close to the critical point, all these indicators are identical to the density and describe the exact same thermodynamic behavior. In this respect, the liquid−liquid transition of water can be equally well described as a transition driven by density or a transition driven by a change in the structural properties.

Since in proximity of the LLCP most of the indicators behave exactly the same as density, to understand the LLT of supercooled water from a thermodynamic viewpoint there is in principle no necessity for a two-order-parameter description of the free energy. Concurrently, there is no loss in information nor accuracy in using such order parameters as an alternative to density, if density is expressed as a linear combination of the fraction of molecules of each type. Moving away from the critical point, the noncritical standard component of the free energy becomes dominant. Correlations between density and structural indicators progressively degrade (but less for Ψ), and specifying the density alone is not sufficient anymore to completely describe the structure of the liquid.

We have also shown that the newly proposed indicator Ψ outperforms all other structural indicators in its ability to identify the local environment of each molecule (Figure 5). While in the low-density liquid, molecules at chemical distance $D = 4$ (distance measured in units of hydrogen bonds) are quite far (relative distance about 6−6.5 Å), in the HDL, the hydrogen bond network folds in, bringing the $D = 4$ molecule into the first shell of the selected molecule (relative distance about 3−3.5 Å).

A study related to our work[78] has appeared during the review process, focusing on some of the indicators discussed herein, as well as on additional structural parameters based on the Delaunay tesselation. They observe that, besides LSI, also the volume and aspect ratio of Delaunay tetrahedra express bimodality close to the critical point, but only with a weak correlation to the system density.

The study of structural indicators has provided great insight into the microscopic behavior of water, and with more and more descriptors becoming available in recent years, our understanding of the local structures of the two liquid states is continuously increasing. We have now a clear picture of the tight coupling that the critical phenomenon enforces between many, apparently distinct, structural properties, where a small fluctuation in any one of these, will be accompanied by a concerted response in all of the others. It is thus foreseeable that several of these indicators can be chosen to numerically investigate nucleation of one liquid into the other with a global order parameter; but studies based on a molecular description (more appropriate to investigate nucleation) should possibly rely on indicators showing unambiguous molecular-level bimodality, such as Ψ. The evidence of a tight coupling between several different structural properties close to the critical point requires a further effort to identify and visualize the structural changes that simultaneously require an increase in density, node total communicability, and V_4 and a decrease in the distance of the fifth neighbor d_5, in the LSI, in tetrahedrality (q_4), in ζ, Ψ, and $\mathcal{H}_c$, and so on.

ASSOCIATED CONTENT

Data Availability Statement

The data that support the findings of this study are available within the article. Additional data (MD trajectories) are available from the corresponding author upon reasonable request.

Supporting Information

The Supporting Information is available free of charge at https://pubs.acs.org/doi/10.1021/acs.jpcb.2c07169.

Description of the new indicator Ψ, analysis of the behavior of LSI (PDF)

AUTHOR INFORMATION

Corresponding Author

Francesco Sciortino − *Dipartimento di Fisica, Sapienza Università di Roma, I-00185 Rome, Italy;* orcid.org/0000-0002-2418-2713; Email: francesco.sciortino@uniroma1.it

Author

Riccardo Foffi − *Institute for Environmental Engineering, Department of Civil, Environmental and Geomatic Engineering, ETH Zürich, 8093 Zürich, Switzerland;* orcid.org/0000-0001-9568-0480

https://doi.org/10.1021/acs.jpcb.2c07169
J. Phys. Chem. B XXXX, XXX, XXX−XXX

Complete contact information is available at:
https://pubs.acs.org/10.1021/acs.jpcb.2c07169

Notes

The authors declare no competing financial interest.

■ ACKNOWLEDGMENTS

We dedicate this article to Pablo Debenedetti, the world expert on metastable liquids, on the occasion of his 70th birthday. F.S. acknowledges support from MIUR-PRIN (Grant No. 2017Z55KCW). We thank Cineca Iscr-B (NNPROT) for computational resources. We wish to thank Isabella Daidone, Chiara Faccio, and Laura Zanetti-Polzi for evaluation of the NTC and Andreas Neophytou for the evaluation of the centreline helicity on the simulation trajectories we provided them.

■ REFERENCES

(1) Gallo, P.; Amann-Winkel, K.; Angell, C. A.; Anisimov, M. A.; Caupin, F.; Chakravarty, C.; Lascaris, E.; Loerting, T.; Panagiotopoulos, A. Z.; Russo, J.; et al. Water: A Tale of Two Liquids. *Chem. Rev.* **2016**, *116*, 7463−7500.
(2) Skinner, L. B.; Galib, M.; Fulton, J. L.; Mundy, C. J.; Parise, J. B.; Pham, V.-T.; Schenter, G. K.; Benmore, C. J. The Structure of Liquid Water up to 360 MPa from X-Ray Diffraction Measurements Using a High Q-range and from Molecular Simulation. *J. Chem. Phys.* **2016**, *144*, 134504.
(3) Debenedetti, P. G. Supercooled and Glassy Water. *J. Phys.: Condens. Matter* **2003**, *15*, R1669.
(4) Loerting, T.; Winkel, K.; Seidl, M.; Bauer, M.; Mitterdorfer, C.; Handle, P. H.; Salzmann, C. G.; Mayer, E.; Finney, J. L.; Bowron, D. T. How many amorphous ices are there? *Phys. Chem. Chem. Phys.* **2011**, *13*, 8783−8794.
(5) Handle, P. H.; Loerting, T.; Sciortino, F. Supercooled and Glassy Water: Metastable Liquid(s), Amorphous Solid(s), and a No-Man's Land. *Proc. Natl. Acad. Sci. U.S.A.* **2017**, *114*, 13336−13344.
(6) Mishima, O.; Calvert, L. D.; Whalley, E. 'Melting Ice' I at 77 and 10 Kbar: A New Method of Making Amorphous Solids. *Nature* **1984**, *310*, 393−395.
(7) Mishima, O.; Calvert, L. D.; Whalley, E. An Apparently First-Order Transition between Two Amorphous Phases of Ice Induced by Pressure. *Nature* **1985**, *314*, 76−78.
(8) Handle, P. H.; Loerting, T. Experimental Study of the Polyamorphism of Water. I. The Isobaric Transitions from Amorphous Ices to LDA at 4 MPa. *J. Chem. Phys.* **2018**, *148*, 124508.
(9) Poole, P. H.; Sciortino, F.; Essmann, U.; Stanley, H. E. Phase Behaviour of Metastable Water. *Nature* **1992**, *360*, 324−328.
(10) Johari, G. P.; Teixeira, J. Thermodynamic Analysis of the Two-Liquid Model for Anomalies of Water, HDL-LDL Fluctuations, and Liquid-Liquid Transition. *J. Phys. Chem. B* **2015**, *119*, 14210−14220.
(11) Soper, A. K. Is Water One Liquid or Two? *J. Chem. Phys.* **2019**, *150*, 234503.
(12) Amann-Winkel, K.; Gainaru, C.; Handle, P. H.; Seidl, M.; Nelson, H.; Bohmer, R.; Loerting, T. Water's Second Glass Transition. *Proc. Natl. Acad. Sci. U.S.A.* **2013**, *110*, 17720−17725.
(13) Stern, J. N.; Seidl-Nigsch, M.; Loerting, T. Evidence for High-Density Liquid Water between 0.1 and 0.3 GPa near 150 K. *Proc. Natl. Acad. Sci. U.S.A.* **2019**, *116*, 9191−9196.
(14) Kim, K. H.; Amann-Winkel, K.; Giovambattista, N.; Späh, A.; Perakis, F.; Pathak, H.; Parada, M. L.; Yang, C.; Mariedahl, D.; Eklund, T.; et al. Experimental Observation of the Liquid-Liquid Transition in Bulk Supercooled Water under Pressure. *Science* **2020**, *370*, 978−982.
(15) Kim, K. H.; Späh, A.; Pathak, H.; Perakis, F.; Mariedahl, D.; Amann-Winkel, K.; Sellberg, J. A.; Lee, J. H.; Kim, S.; Park, J.; et al. Maxima in the Thermodynamic Response and Correlation Functions of Deeply Supercooled Water. *Science* **2017**, *358*, 1589−1593.
(16) Kringle, L.; Thornley, W. A.; Kay, B. D.; Kimmel, G. A. Reversible Structural Transformations in Supercooled Liquid Water from 135 to 245 K. *Science* **2020**, *369*, 1490−1492.
(17) Sciortino, F.; La Nave, E.; Tartaglia, P. Physics of the liquid-liquid critical point. *Physical review letters* **2003**, *91*, 155701.
(18) Abascal, J. L.; Vega, C. Widom line and the liquid-liquid critical point for the TIP4P/2005 water model. *J. Chem. Phys.* **2010**, *133*, 234502.
(19) Li, Y.; Li, J.; Wang, F. Liquid−liquid transition in supercooled water suggested by microsecond simulations. *Proc. Natl. Acad. Sci. U. S. A.* **2013**, *110*, 12209−12212.
(20) Yagasaki, T.; Matsumoto, M.; Tanaka, H. Spontaneous liquid-liquid phase separation of water. *Phys. Rev. E* **2014**, *89*, 020301.
(21) Ni, Y.; Skinner, J. Evidence for a liquid-liquid critical point in supercooled water within the E3B3 model and a possible interpretation of the kink in the homogeneous nucleation line. *J. Chem. Phys.* **2016**, *144*, 214501.
(22) Gartner, T. E.; Zhang, L.; Piaggi, P. M.; Car, R.; Panagiotopoulos, A. Z.; Debenedetti, P. G. Signatures of a Liquid−Liquid Transition in an Ab Initio Deep Neural Network Model for Water. *Proc. Natl. Acad. Sci. U.S.A.* **2020**, *117*, 26040.
(23) Eltareb, A.; Lopez, G. E.; Giovambattista, N. Evidence of a Liquid- Liquid Phase Transition in H$$_2$$O and D$$_2$$O from Path-Integral Molecular Dynamics Simulations. *Sci. Rep.* **2022**, *12*, 6004.
(24) Liu, Y.; Panagiotopoulos, A. Z.; Debenedetti, P. G. Low-Temperature Fluid-Phase Behavior of ST2 Water. *J. Chem. Phys.* **2009**, *131*, 104508.
(25) Sciortino, F.; Saika-Voivod, I.; Poole, P. H. Study of the ST2Model of Water Close to the Liquid-Liquid Critical Point. *Phys. Chem. Chem. Phys.* **2011**, *13*, 19759.
(26) Kesselring, T. A.; Franzese, G.; Buldyrev, S. V.; Herrmann, H. J.; Stanley, H. E. Nanoscale dynamics of phase flipping in water near its hypothesized liquid-liquid critical point. *Sci. Rep.* **2012**, *2*, 474.
(27) Palmer, J. C.; Martelli, F.; Liu, Y.; Car, R.; Panagiotopoulos, A. Z.; Debenedetti, P. G. Metastable Liquid-Liquid Transition in a Molecular Model of Water. *Nature* **2014**, *510*, 385−388.
(28) Palmer, J. C.; Poole, P. H.; Sciortino, F.; Debenedetti, P. G. Advances in Computational Studies of the Liquid-Liquid Transition in Water and Water-Like Models. *Chem. Rev.* **2018**, *118*, 9129−9151.
(29) Debenedetti, P. G.; Sciortino, F.; Zerze, G. H. Second Critical Point in Two Realistic Models of Water. *Science* **2020**, *369*, 289−292.
(30) Weis, J.; Sciortino, F.; Panagiotopoulos, A. Z.; Debenedetti, P. G. Liquid-Liquid Criticality in the WAIL Water Model. *J. Chem. Phys.* **2022**, *157*, 024502.
(31) Hsu, C. W.; Largo, J.; Sciortino, F.; Starr, F. W. Hierarchies of networked phases induced by multiple liquid−liquid critical points. *Proc. Natl. Acad. Sci. U. S. A.* **2008**, *105*, 13711−13715.
(32) Smallenburg, F.; Filion, L.; Sciortino, F. Erasing No-Man's Land by Thermodynamically Stabilizing the Liquid-Liquid Transition in Tetrahedral Particles. *Nat. Phys.* **2014**, *10*, 653−657.
(33) Ciarella, S.; Gang, O.; Sciortino, F. Toward the observation of a liquid-liquid phase transition in patchy origami tetrahedra: a numerical study. *Eur. Phys. J. E* **2016**, *39*, 131.
(34) Neophytou, A.; Chakrabarti, D.; Sciortino, F. Topological nature of the liquid-liquid phase transition in tetrahedral liquids. *Nat. Phys.* **2022**, *18*, 1248.
(35) Tanaka, H. Simple Physical Model of Liquid Water. *J. Chem. Phys.* **2000**, *112*, 799−809.
(36) Cuthbertson, M. J.; Poole, P. H. Mixturelike Behavior Near a Liquid-Liquid Phase Transition in Simulations of Supercooled Water. *Phys. Rev. Lett.* **2011**, *106*, 115706.
(37) Holten, V.; Anisimov, M. A. Entropy-Driven Liquid-Liquid Separation in Supercooled Water. *Sci. Rep.* **2012**, *2*, 713.
(38) Anisimov, M. A.; Duška, M.; Caupin, F.; Amrhein, L. E.; Rosenbaum, A.; Sadus, R. J. Thermodynamics of Fluid Polymorphism. *Phys. Rev. X* **2018**, *8*, 011004.
(39) Singh, R. S.; Biddle, J. W.; Debenedetti, P. G.; Anisimov, M. A. Two-State Thermodynamics and the Possibility of a Liquid-Liquid

Phase Transition in Supercooled TIP4P/2005 Water. *J. Chem. Phys.* **2016**, *144*, 144504.
(40) Biddle, J. W.; Singh, R. S.; Sparano, E. M.; Ricci, F.; González, M. A.; Valeriani, C.; Abascal, J. L. F.; Debenedetti, P. G.; Anisimov, M. A.; Caupin, F. Two-Structure Thermodynamics for the TIP4P/2005 Model of Water Covering Supercooled and Deeply Stretched Regions. *J. Chem. Phys.* **2017**, *146*, 034502.
(41) Caupin, F.; Anisimov, M. A. Minimal Microscopic Model for Liquid Polyamorphism and Waterlike Anomalies. *Phys. Rev. Lett.* **2021**, *127*, 185701.
(42) Moynihan, C. T. Two species/nonideal solution model for amorphous/amorphous phase transitions. *MRS Online Proceedings Library (OPL)* **1996**, *455*, 411−425.
(43) Ponyatovsky, E.; Sinitsyn, V.; Pozdnyakova, T. The metastable T- p phase diagram and anomalous thermodynamic properties of supercooled water. *J. Chem. Phys.* **1998**, *109*, 2413−2422.
(44) Errington, J. R.; Debenedetti, P. G. Relationship between Structural Order and the Anomalies of Liquid Water. *Nature* **2001**, *409*, 318−321.
(45) Shiratani, E.; Sasai, M. Growth and Collapse of Structural Patterns in the Hydrogen Bond Network in Liquid Water. *J. Chem. Phys.* **1996**, *104*, 7671−7680.
(46) Russo, J.; Tanaka, H. Understanding Water's Anomalies with Locally Favoured Structures. *Nat. Commun.* **2014**, *5*, 3556.
(47) Tanaka, H.; Tong, H.; Shi, R.; Russo, J. Revealing Key Structural Features Hidden in Liquids and Glasses. *Nat. Rev. Phys.* **2019**, *1*, 333−348.
(48) Montes de Oca, J. M.; Sciortino, F.; Appignanesi, G. A. A Structural Indicator for Water Built upon Potential Energy Considerations. *J. Chem. Phys.* **2020**, *152*, 244503.
(49) Muthachikavil, A. V.; Kontogeorgis, G. M.; Liang, X.; Lei, Q.; Peng, B. Structural Characteristics of Low-Density Environments in Liquid Water. *Phys. Rev. E* **2022**, *105*, 034604.
(50) Martelli, F. Unravelling the Contribution of Local Structures to the Anomalies of Water: The Synergistic Action of Several Factors. *J. Chem. Phys.* **2019**, *150*, 094506.
(51) Foffi, R.; Russo, J.; Sciortino, F. Structural and Topological Changes across the Liquid-Liquid Transition in Water. *J. Chem. Phys.* **2021**, *154*, 184506.
(52) Foffi, R.; Sciortino, F. Structure of High-Pressure Supercooled and Glassy Water. *Phys. Rev. Lett.* **2021**, *127*, 175502.
(53) Faccio, C.; Benzi, M.; Zanetti-Polzi, L.; Daidone, I. Low- and High-Density Forms of Liquid Water Revealed by a New Medium-Range Order Descriptor. *J. Mol. Liq.* **2022**, *355*, 118922.
(54) Duboué-Dijon, E.; Laage, D. Characterization of the Local Structure in Liquid Water by Various Order Parameters. *J. Phys. Chem. B* **2015**, *119*, 8406−8418.
(55) Shi, R.; Tanaka, H. Microscopic Structural Descriptor of Liquid Water. *J. Chem. Phys.* **2018**, *148*, 124503.
(56) Stanley, H. E.*Introduction to Phase Transitions and Critical Phenomena*; Oxford University Press: New York, 1987.
(57) Abascal, J. L. F.; Sanz, E.; García Fernández, R.; Vega, C. A Potential Model for the Study of Ices and Amorphous Water: TIP4P/Ice. *J. Chem. Phys.* **2005**, *122*, 234511.
(58) Abraham, M. J.; Murtola, T.; Schulz, R.; Páll, S.; Smith, J. C.; Hess, B.; Lindahl, E. GROMACS: High Performance Molecular Simulations through Multi-Level Parallelism from Laptops to Supercomputers. *SoftwareX* **2015**, *1−2*, 19−25.
(59) Frenkel, D.; Smit, B.*Understanding Molecular Simulation from Algorithms to Applications*; Academic Press: San Diego, 2002.
(60) Parrinello, M.; Rahman, A. Polymorphic Transitions in Single Crystals: A New Molecular Dynamics Method. *J. Appl. Phys.* **1981**, *52*, 7182−7190.
(61) Hess, B.; Bekker, H.; Berendsen, H. J. C.; Fraaije, J. G. E. M. LINCS: A Linear Constraint Solver for Molecular Simulations. *J. Comput. Chem.* **1997**, *18*, 1463−1472.
(62) Allen, M. P.; Tildesley, D. J.*Computer Simulation of Liquids*, second ed.; Oxford University Press: Oxford, 2017.
(63) Stillinger, F. H.*Energy Landscapes, Inherent Structures, and Condensed-Matter Phenomena*; Princeton University Press: Princeton, NJ, 2015.
(64) Luzar, A.; Chandler, D. Hydrogen-Bond Kinetics in Liquid Water. *Nature* **1996**, *379*, 55−57.
(65) Foffi, R.Psi_StructuralIndicator.jl. *GitHub repository*2022, https://github.com/mastrof/Psi_StructuralIndicator.jl.
(66) Parzen, E. On Estimation of a Probability Density Function and Mode. *Ann. Math. Stat.* **1962**, *33*, 1065−1076.
(67) Massey, F. J. The Kolmogorov-Smirnov Test for Goodness of Fit. *J. Am. Stat. Assoc.* **1951**, *46*, 68−78.
(68) Appignanesi, G. A.; Rodriguez Fris, J. A.; Sciortino, F. Evidence of a two-state picture for supercooled water and its connections with glassy dynamics. *Eur. Phys. J. E* **2009**, *29*, 305−310.
(69) Gelman Constantin, J.; Rodriguez Fris, A.; Appignanesi, G.; Carignano, M.; Szleifer, I.; Corti, H. Structure of supercooled water in clusters and bulk and its relation to the two-state picture of water: Results from the TIP4P-ice model. *Eur. Phys. J. E* **2011**, *34*, 126.
(70) Wikfeldt, K. T.; Nilsson, A.; Pettersson, L. G. M. Spatially Inhomogeneous Bimodal Inherent Structure of Simulated Liquid Water. *Phys. Chem. Chem. Phys.* **2011**, *13*, 19918.
(71) Accordino, S. R.; Rodriguez Fris, J. A.; Sciortino, F.; Appignanesi, G. A. Quantitative investigation of the two-state picture for water in the normal liquid and the supercooled regime. *Eur. Phys. J. E Soft Matter* **2011**, *34*, 48.
(72) Callen, H. B.; Callen, H. B.*Thermodynamics and an Introduction to Thermostatistics*, 2nd ed.; Wiley: New York, 1985.
(73) Gallo, P.; Sciortino, F. Ising Universality Class for the Liquid-Liquid Critical Point of a One Component Fluid: A Finite-Size Scaling Test. *Phys. Rev. Lett.* **2012**, *109*, 177801.
(74) Wilding, N. B.; Bruce, A. D. Density Fluctuations and Field Mixing in the Critical Fluid. *J. Phys.: Condens. Matter* **1992**, *4*, 3087−3108.
(75) Tanaka, H. Two-Order-Parameter Description of Liquids: Critical Phenomena and Phase Separation of Supercooled Liquids. *J. Phys.: Condens. Matter* **1999**, *11*, L159−L168.
(76) Cerdeiriña, C. A.; Troncoso, J.; González-Salgado, D.; Debenedetti, P. G.; Stanley, H. E. Water's Two-Critical-Point Scenario in the Ising Paradigm. *J. Chem. Phys.* **2019**, *150*, 244509.
(77) Tanaka, H. Liquid−Liquid Transition and Polyamorphism. *J. Chem. Phys.* **2020**, *153*, 130901.
(78) Škvára, J.; Nezbeda, I. Liquid−Liquid Transition and Polyamorphism. *J. Mol. Liq.* **2022**, *367*, 120508.

https://doi.org/10.1021/acs.jpcb.2c07169
J. Phys. Chem. B XXXX, XXX, XXX−XXX